applied biosciences

MDPI

Article

Immunocapture RT-qPCR Method for DWV-A Surveillance: Eliminating Hazardous Extraction for Screening Applications

Krisztina Christmon [1,*], Eugene V. Ryabov [2,3], James Tauber [2] and Jay D. Evans [2]

[1] Plant Sciences Building, Department of Entomology, University of Maryland, 4291 Fieldhouse Drive, College Park, MD 20742, USA
[2] USDA-ARS Bee Research Laboratory, BARC-East Building 306, Beltsville, MD 20705, USA; eugene.ryabov@hutton.ac.uk (E.V.R.); jay.evans@usda.gov (J.D.E.)
[3] The James Hutton Institute, Invergowrie, Dundee DD2 5DA, UK
* Correspondence: krisztina.christmon@gmail.com; Tel.: +1-(301)-237-9390

Abstract

Deformed wing virus (DWV) is a major contributor to honey bee colony losses, making effective monitoring essential for apiary management. Traditional DWV detection relies on hazardous RNA extraction followed by RT-qPCR, creating barriers for widespread surveillance. We developed an immunocapture RT-qPCR (IC-RT-PCR) method for screening DWV-A infections by capturing intact virus particles from bee homogenates using immobilized antibodies. Validation demonstrated strong correlation with TRIzol®-based extraction (r = 0.821), with approximately 6 Ct reduced sensitivity, consistent with other published immunocapture methods. Performance was adequate for moderate–high viral loads, while TRIzol® showed superior detection for low-dose infections. Laboratory-produced reverse transcriptase showed equivalent performance to commercial enzymes, providing cost savings. IC-RT-PCR eliminates hazardous chemicals and offers a streamlined workflow for surveillance screening where the safety and cost benefits outweigh the sensitivity reduction. This method provides a practical alternative for large-scale DWV-A surveillance programs, while TRIzol® remains preferable for low-level detection and diagnostic confirmation.

Keywords: virus; honey bee; deformed wing virus; RT-qPCR; insect pollinator health

check for updates

Academic Editor: Spiros Paramithiotis

Received: 21 April 2025
Revised: 23 July 2025
Accepted: 30 July 2025
Published: 6 August 2025

Citation: Christmon, K.; Ryabov, E.V.; Tauber, J.; Evans, J.D. Immunocapture RT-qPCR Method for DWV-A Surveillance: Eliminating Hazardous Extraction for Screening Applications. *Appl. Biosci.* **2025**, *4*, 40. https://doi.org/10.3390/applbiosci4030040

Copyright: © 2025 by the authors. Licensee MDPI, Basel, Switzerland. This article is an open access article distributed under the terms and conditions of the Creative Commons Attribution (CC BY) license (https://creativecommons.org/licenses/by/4.0/).

1. Introduction

Deformed wing virus (DWV) [1] is a pathogen affecting the western honey bee (*Apis mellifera* L.) which significantly affects colony health and survival [2–5]. DWV is pervasive and present in the majority of honey bee colonies, particularly in regions where the parasitic mite *Varroa destructor* is prevalent. The impact becomes particularly detrimental through the synergistic relationship between the virus and mite, where mite feeding both transmits the virus and suppresses bee immunity, leading to increased viral replication and consequently higher bee mortality [6]. Understanding and monitoring DWV prevalence and load has therefore become essential for effective colony health management and sustainable beekeeping practices.

1.1. Current Detection Methods and Limitations

The current standard for assessing DWV levels involves extracting total RNA from honey bee tissues using an acid-phenol protocol, such as TRIzol® (Invitrogen, Carlsbad, CA, USA), herein referred to simply as the "TRIzol®" method [7]. This RNA is then quantified using reverse-transcription quantitative polymerase chain reaction (RT-qPCR). While this

method provides precise quantification of the viral load, it presents several practical barriers for large-scale surveillance:

Safety and Infrastructure Concerns: The use of phenol-chloroform extraction requires specialized laboratory infrastructure, including fume hoods and hazardous waste disposal systems. These chemicals pose substantial health risks to laboratory personnel and create regulatory compliance challenges for institutions conducting large-scale screening. For field-based surveillance programs or laboratories in resource-limited settings, these requirements can be prohibitive.

Cost Considerations: Beyond the direct costs of hazardous reagents, TRIzol®-based extraction incurs substantial indirect expenses, including specialized safety equipment, waste disposal fees, and extended processing times. For surveillance programs requiring analysis of hundreds or thousands of samples, these costs can become economically unfeasible.

Throughput Limitations: The multi-step nature of RNA extraction, including phase separation, precipitation, and purification steps, limits sample processing throughput and increases opportunities for cross-contamination. These constraints are particularly problematic for time-sensitive surveillance applications, where rapid results are needed for management decisions.

1.2. Immunocapture Approaches: Established Alternative Strategy

Immunocapture techniques have been successfully employed for viral detection in various pathosystems, offering simplified sample preparation, while maintaining analytical specificity. The basic principle involves using immobilized antibodies to selectively capture viral particles from complex sample matrices, followed by direct molecular analysis of the captured material [8]. This approach has demonstrated particular success for plant virus detection, where it enables field-deployable diagnostic systems with reduced infrastructure requirements.

Published immunocapture methods for viruses including Indian citrus ringspot virus [9], Potato Mop-Top Virus [10], and others [11] have consistently demonstrated similar performance characteristics: strong correlation with standard extraction methods, accompanied by 5–10 Ct reduced sensitivity. This sensitivity trade-off is well established and accepted in exchange for practical advantages including improved safety, reduced costs, and simplified workflows.

The adaptation of immunocapture methods to honey bee viral diagnostics follows established principles, while addressing the unique challenges of bee homogenates, which contain high levels of proteins, lipids, and other potential interferents. The requirement for quantitative results necessitates careful validation to ensure that capture efficiency remains consistent across varying viral loads and sample conditions.

1.3. DWV Biology and Detection Challenges

DWV exists as a complex of related viral variants, with DWV-A and DWV-B representing the most epidemiologically significant strains [12]. These variants differ in their pathogenicity profiles and geographic distribution [13]. The viral load in infected bees can vary dramatically depending on factors including mite burden, bee age, season, and colony health status, creating detection challenges across a wide dynamic range [4,14].

Developmental Stage Considerations: Viral loads differ significantly between bee life stages, with pupae and newly emerged adults often showing distinct infection profiles [15]. This biological variability necessitates validation of detection methods across developmental stages to ensure reliable performance in field applications where mixed-age populations are commonly sampled.

Infection Route Dependencies: Natural DWV infections typically occur through mite-mediated transmission or horizontal transfer between bees, resulting in different tissue distribution patterns compared to experimental infections [6,16]. Understanding how detection methods perform across different infection scenarios is crucial for appropriate application in surveillance programs.

1.4. Method Positioning and Practical Applications

This study presents the development and validation of an immunocapture RT-qPCR method specifically designed for DWV-A surveillance applications where practical advantages outweigh the expected sensitivity reduction typical of immunocapture approaches. Rather than seeking to replace established extraction methods, this work expands the available toolkit for different surveillance scenarios.

The concept is to provide a complementary method that sacrifices some analytical sensitivity in exchange for improved safety, simplified workflows, and reduced infrastructure requirements. Some operations may find that this approach provides sufficient information for management decisions, while retaining the option to use more sensitive methods for samples requiring precise quantification or confirmation of low-level infections.

1.5. Research Objectives

This study aimed to develop and validate an immunocapture protocol that eliminates hazardous RNA extraction for DWV-A detection, while honestly assessing performance against the TRIzol® standard. The specific objectives included

1. Develop and validate an immunocapture protocol for DWV-A detection following established immunocapture principles.
2. Evaluate laboratory-produced reverse transcriptase as a cost-effective alternative to commercial enzymes.
3. Characterize method performance across different viral loads, infection routes, and bee life stages.
4. Define practical applications where the method provides useful information despite expected sensitivity limitations.
5. Establish clear guidelines for appropriate method selection based on application requirements.

1.6. Study Design and Validation Philosophy

Our validation strategy focused on defining specific scenarios where immunocapture provides useful information, while clearly acknowledging the sensitivity limitations typical of this approach. The study emphasizes rigorous statistical validation using appropriate normality testing and statistical test selection, with results interpreted in the context of published immunocapture literature, rather than attempting to compete directly with gold standard extraction methods.

We developed a comprehensive validation protocol including paired comparisons between methods, assessment across different infection routes and viral loads, and evaluation of method performance with laboratory-produced versus commercial reagents. This approach ensures that the conclusions accurately reflect method capabilities within the expectations established for immunocapture approaches.

2. Materials and Methods

2.1. Antiserum Production and Characterization

Polyclonal rabbit antiserum against DWV was produced as previously described [17], following methods initially described by Clark and Adams (1977) [8] and employing

a modified protocol based on Mumford and Seal (1997) [12]. Antibody specificity was validated by Western blot analysis using identical antisera, confirming specific recognition of DWV structural proteins [17]. The antisera were diluted fourfold with PBS and pre-absorbed using acetone powder prepared from Varroa-free honey bee pupae containing baseline DWV levels (below 10^4 genome equivalents per pupa, determined by RT-qPCR) to reduce cross-reactivity with host proteins [18].

2.2. Reverse Transcriptase Evaluation and Selection

Two reverse transcriptases were evaluated for equivalency before method validation:
Commercial SuperScript II (Thermo Fisher): Used according to the manufacturer's protocols.

Laboratory-produced reverse transcriptase (Mashup RTase [19]): The laboratory-produced reverse transcriptase was prepared as follows:

Transformation and Protein Expression: A dried plasmid encoding the Mashup RTase was rehydrated in TE elution buffer at 60 °C. BL21(DE3) Competent E. coli (NEB) was transformed with 5 µL of the rehydrated plasmid and plated on LB with 50 µg/mL kanamycin. Following overnight incubation at 37 °C, a single colony was selected and grown in 10 mL LB with 50 µg/mL kanamycin at 30 °C overnight. The next day, 3 mL of the seed culture was inoculated into 300 mL LB with 50 µg/mL kanamycin and grown at 37 °C with 220 rpm shaking for approximately 2 h. The shaker temperature was then reduced to 25 °C, and protein expression was induced by adding 0.5 mM IPTG. The culture continued incubation overnight at 25 °C.

Cell Lysis and Protein Purification: After approximately 24 h of induction, cells were harvested by centrifugation at 5000 rpm at 4 °C. Cell pellets were resuspended in lysis buffer (300 mM NaCl, 25 mM Tris-HCl pH 7.5, 10% glycerol, 0.5% Triton X-100) with lysozyme powder, protease inhibitor tablet, and TURBO DNase. After 40 min of incubation at 25 °C, the lysate was centrifuged and the supernatant purified using NEBExpress™ Ni Spin Columns according to the manufacturer's protocol. The purified enzyme was concentrated and buffer-exchanged, with final storage at −20 °C in buffer containing 50% glycerol.

2.3. Reagents and Solutions

Phosphate-buffered saline (PBS) was prepared using 137 mM NaCl, 2.7 mM KCl, 10 mM Na_2HPO_4, and 1.8 mM KH_2PO_4, adjusted to pH 7.4. All solutions were prepared using molecular-biology-grade reagents and nuclease-free water. PBS-Tween (PBS-T) was prepared by adding Tween-20 to PBS at a final concentration of 0.05%.

2.4. Sample Collection and Preparation

Newly emerged worker bees and worker bee pupae were collected from a Varroa-infested honey bee colony at the USDA-ARS apiary in Beltsville, MD, USA. Individual bees were screened for the presence of *V. destructor* mites, and non-parasitized individuals were selected for experiments.

Homogenate Preparation: Individual bees/pupae were homogenized in 0.5 mL PBS using sterile pestles in 1.5 mL microcentrifuge tubes (approximately 1 min on ice), followed by centrifugation at 8000× *g* for 5 min. Homogenates were filtered to remove debris (filter specifications: 0.45 µm cellulose acetate filters, Millipore).

Note on Standardization: Samples were standardized by individual bee/pupa rather than by tissue weight or protein content. While this may contribute to variability between samples from different developmental stages, it reflects typical field surveillance conditions where individual bee assessment is standard practice.

2.5. Experimental Design

Experiment 1: Antisera Dilution Optimization

- Comparison of 1:1000 and 1:100 dilutions vs. no antisera control
- Evaluation using qPCR Ct values from naturally infected bees

Experiment 2A: Pre-absorption Evaluation

- Comparison of pre-absorbed vs. non-treated antisera
- Assessment of background reduction effectiveness

Experiment 2B: Reverse Transcriptase Validation

- Direct comparison of commercial SuperScript II vs. laboratory-produced reverse transcriptase
- Confirmation of equivalent performance before method validation

Experiment 3: Method Validation Against TRIzol® Standard

- Direct comparison using paired samples across viral load ranges
- Assessment across bee life stages (pupae vs. newly emerged bees)

Experiment 4: Route-Dependent Performance Assessment

- Comparison of oral vs. injection infection detection
- Evaluation of viral load thresholds for method applicability

2.6. Infection Protocols

Pupal Injection Experiments: Purple-eye stage pupae were carefully removed from frames containing capped brood. Each pupa received a lateral microinjection of 10 µL containing 10^4 DWV copies in PBS under the third abdominal sternite. Injected pupae were maintained in Petri dishes with folded filter paper at 37 °C and approximately 50% relative humidity.

Oral Infection Experiments: Newly emerged worker bees were starved for 2 h before receiving 10 µL doses of either 1:1 DWV–sugar water solution (10^7 or 10^8 genome equivalents) or control solution (1:2 sugar–water).

Adult Injection Experiments: Newly emerged workers were injected with 10 µL of either PBS control, 10^4 genome equivalents of DWV, or 10^6 genome equivalents of DWV.

Five days post-treatment, bees were individually homogenized in 100 µL of PBS using a sterile pestle in 1.5 mL microcentrifuge tubes.

2.7. Immunocapture Protocol

Ninety-six-well qPCR plates (Bio-Rad) were coated with 100 µL of 1:250 diluted pre-absorbed polyclonal anti-DWV rabbit antiserum in 0.05 M sodium carbonate buffer (pH 9.6). After 2 h incubation at 37 °C, solutions were carefully removed using an 8-channel pipettor, avoiding contact with well walls to preserve the antibody coating. Wells were washed three times with PBS-T (PBS + 0.05% Tween-20).

Sample Loading: 50 µL of cleared bee extract was combined with 150 µL PBS-T per well. Plates were incubated at 4 °C for 18 h to maximize viral particle capture.

Viral Particle Lysis and RNA Release: Following immunocapture, viral particles were lysed to release RNA for cDNA synthesis. Nuclease-free water (pre-heated to 90 °C) was quickly pipetted (11.9 µL) into each well to denature viral proteins and release genomic RNA. Plates were incubated at 70 °C for 5 min to ensure complete particle disruption, followed by brief centrifugation and placement on ice.

2.8. Molecular Analysis

Reverse Transcription: For cDNA synthesis, each well received 11 µL nuclease-free water, 1 µL dNTP mix (10 mM each), and 1 µL random primer (100 ng/µL). Plates were sealed, mixed, briefly centrifuged, heated at 65 °C for 5 min, and placed on ice. The reaction mixture was completed by adding 4 µL 5× Buffer, 2 µL 0.1 M DTT, 1 µL RNase inhibitor (RNAse Out, Thermo Fisher), and 1 µL reverse transcriptase (either SuperScript II or laboratory-produced). Reactions were incubated at 25 °C for 10 min, 42 °C for 50 min, 70 °C for 10 min, and held at 10 °C.

Quantitative PCR: The cDNA was diluted tenfold with 180 µL nuclease-free water per well. qPCR reactions (20 µL total volume) contained 2.0 µL diluted cDNA, 10 µL SYBR Green (SsoAdvanced Universal SYBR Green Supermix, Bio-Rad, Hercules, CA, USA), 0.4 µL each of forward (5′-GAGATTGAAGCGCATGAACA-3′) and reverse (5′-TGAATTCAGTGTCGCCCATA-3′) primers (10 µM), and 7.2 µL nuclease-free water.

Cycling conditions: Initial denaturation at 95 °C for 30 s, followed by 49 cycles of 95 °C for 5 s and 60 °C for 30 s. Melt curve analysis included 95 °C for 10 s, 60 °C for 5 s, and 0.5 °C increments every 5 s to 95 °C.

TRIzol® Extraction Comparison: For comparison samples, total RNA was extracted from PBS homogenates using TRIzol® reagent (Thermo Fisher, San Francisco, CA, USA) following established protocols for honey bee samples [7], followed by identical RT-qPCR procedures.

2.9. Statistical Analysis

Data normality was assessed using Shapiro-Wilk tests ($\alpha = 0.05$). For experiments where all groups showed normal distributions ($p > 0.05$), parametric tests were employed: Student's *t*-tests for two-group comparisons and one-way ANOVA followed by Tukey's HSD post hoc tests for multiple comparisons. For experiments where one or more groups showed non-normal distributions ($p \leq 0.05$), non-parametric alternatives were used: Mann–Whitney U tests for two-group comparisons and Kruskal–Wallis tests for multiple group comparisons. Statistical significance was set at $p < 0.05$. All analyses were performed using R version 4.0.2.

3. Results

3.1. Experiment 1: Optimization of Antisera Dilution

We evaluated the effectiveness of different antisera dilutions for immunocapture RT-PCR by comparing 1:1000 (IC.1to1000.AS) and 1:100 (IC.1to100.AS) dilutions of anti-DWV rabbit antiserum against a no-antiserum control (IC.No.AS) (Figure 1, Table 1).

Shapiro–Wilk tests revealed non-normal distributions for the IC.1to1000.AS group ($W = 0.7015$, $p < 0.001$) and TRIzol® group ($W = 0.7135$, $p = 0.001$), while the IC.No.AS ($W = 0.9368$, $p = 0.518$) and IC.1to100.AS ($W = 0.8493$, $p = 0.057$) groups showed normal distributions. Due to the presence of non-normal data, non-parametric analysis was employed.

Kruskal–Wallis analysis showed no significant differences between methods ($H = 1.51$, $df = 3$, $p = 0.680$). The median Ct values were IC.No.AS: 29.1 (IQR: 26.4–30.2), IC.1to1000.AS: 23.2 (IQR: 22.6–35.2), IC.1to100.AS: 28.8 (IQR: 27.5–33.1), and TRIzol®: 14.6 (IQR: 14.3–32.8).

Despite the lack of statistical significance, the 1:1000 dilution showed more consistent performance, with lower variability compared to the 1:100 dilution, making it the optimal choice for the subsequent experiments.

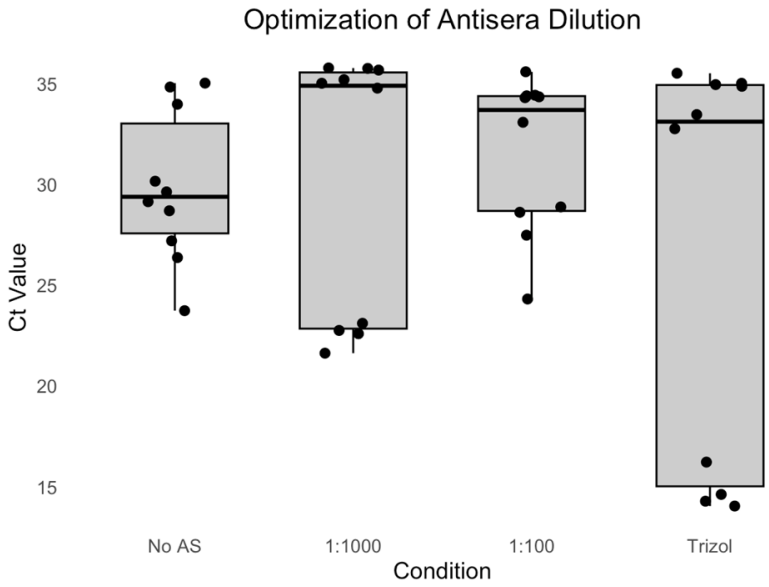


Figure 1. Optimization of antisera dilution for immunocapture RT-qPCR detection of DWV-A. Comparison of cycle threshold (Ct) values obtained using different antisera dilutions for immunocapture and TRIzol® RNA extraction. IC.No.AS: immunocapture without antisera (negative control); IC.1to1000.AS: immunocapture with 1:1000 diluted antisera; IC.1to100.AS: immunocapture with 1:100 diluted antisera; TRIzol®: conventional RNA extraction followed by RT-qPCR. Box plots show median (horizontal line), interquartile range (box), and individual data points are overlaid. Shapiro–Wilk tests revealed non-normal distributions for IC.1to1000.AS and TRIzol® groups ($p < 0.05$), necessitating non-parametric analysis. Kruskal–Wallis test showed no significant differences between methods ($H = 1.51$, $df = 3$, $p = 0.680$). $n = 10$ per group.

Table 1. Antisera dilution optimization for immunocapture RT-qPCR detection of DWV-A. Cycle threshold (Ct) values comparing 1:1000 dilution (IC.1to1000.AS), 1:100 dilution (IC.1to100.AS), no antisera control (IC.No.AS), and TRIzol® extraction.

Sample	IC.No.AS	IC.1to1000.AS	IC.1to100.AS	TRIzol®
1	30.16	23.11	27.48	16.23
2	26.37	21.63	28.62	14.29
3	23.74	22.60	28.88	14.05
4	27.20	22.76	24.32	14.63
5	28.69	35.19	33.08	32.76
6	29.14	35.77	34.39	33.46
7	29.63	35.75	34.34	34.95
8	33.97	35.01	34.30	35.51
9	35.02	35.67	35.58	35.01
10	34.83	34.77	34.42	34.86

3.2. Experiment 2: Evaluation of Pre-Absorbed Antisera and Reverse Transcriptases

3.2.1. Experiment 2a: Comparison of Pre-Absorbed and Non-Treated Antisera

We compared three conditions for immunocapture: no antibody (No.Antibody), pre-absorbed antiserum (PreAbs.Antibody), and non-treated antisera (Antibody) (Figure 2, Table 2).

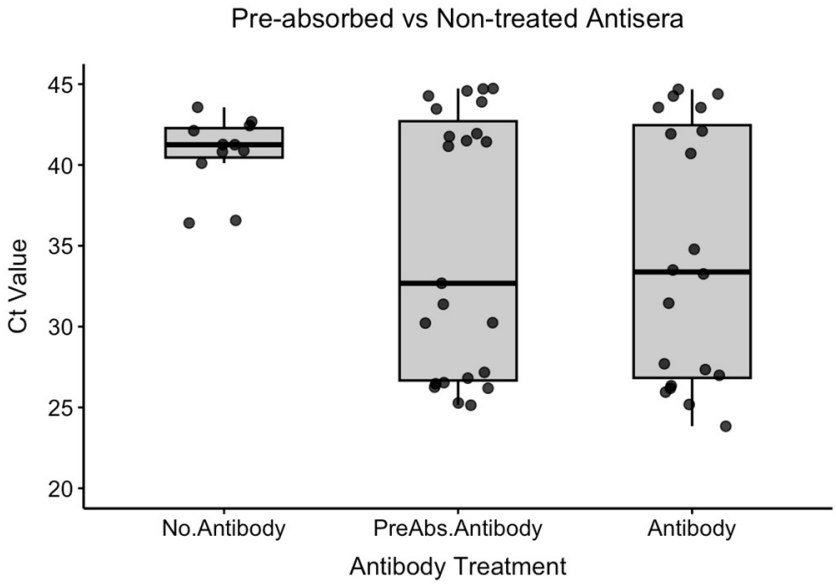


Figure 2. Comparison of pre-absorbed and non-treated antisera for immunocapture RT-qPCR detection of DWV-A. Cycle threshold (Ct) values for three immunocapture conditions: No.Antibody (no antibody control), PreAbs.Antibody (pre-absorbed antisera), and Antibody (non-treated antisera). Box plots show median (horizontal line), interquartile range (box), and individual data points are overlaid. Shapiro–Wilk tests revealed non-normal distributions for PreAbs.Antibody and Antibody groups ($p < 0.05$), necessitating non-parametric analysis. Mann–Whitney U tests showed no significant differences between any pairwise comparisons (all $p > 0.05$). Sample sizes: No.Antibody ($n = 11$), PreAbs.Antibody ($n = 24$), Antibody ($n = 22$).

Table 2. Comparison of qPCR cycle threshold (Ct) values across immunocapture conditions. Mean Ct values and standard deviations are shown for samples treated with no antibody (No.Antibody), pre-absorbed antibody (PreAbs.Antibody), and non-treated antibody (Antibody).

Sample	Condition	Ct Value
1	No.Antibody	36.41
2	No.Antibody	36.57
3	No.Antibody	40.88
4	No.Antibody	40.11
5	PreAbs.Antibody	26.19
6	PreAbs.Antibody	26.53
7	PreAbs.Antibody	25.14
8	PreAbs.Antibody	25.28
9	Antibody	25.95
10	Antibody	25.18
11	Antibody	26.35
12	Antibody	23.84
13	No.Antibody	40.81
14	No.Antibody	41.26
15	No.Antibody	42.12
16	No.Antibody	42.68
17	PreAbs.Antibody	26.81
18	PreAbs.Antibody	27.17
19	PreAbs.Antibody	26.26
20	PreAbs.Antibody	26.47
21	Antibody	26.19
22	Antibody	27.70

Table 2. *Cont.*

Sample	Condition	Ct Value
23	Antibody	26.99
24	Antibody	27.34
25	No.Antibody	41.25
26	No.Antibody	42.44
27	No.Antibody	43.57
28	PreAbs.Antibody	32.68
29	PreAbs.Antibody	31.38
30	PreAbs.Antibody	30.24
31	PreAbs.Antibody	30.22
32	Antibody	31.45
33	Antibody	34.78
34	Antibody	33.50
35	Antibody	33.26
36	PreAbs.Antibody	43.90
37	PreAbs.Antibody	45.78
38	Antibody	49.04
39	Antibody	47.35
40	PreAbs.Antibody	41.76
41	PreAbs.Antibody	41.43
42	PreAbs.Antibody	41.94
43	PreAbs.Antibody	41.16
44	Antibody	40.71
45	Antibody	43.55
46	Antibody	43.56
47	Antibody	44.68
48	PreAbs.Antibody	41.50
49	PreAbs.Antibody	44.58
50	PreAbs.Antibody	44.27
51	Antibody	44.26
52	PreAbs.Antibody	43.47
53	PreAbs.Antibody	44.70
54	PreAbs.Antibody	44.73
55	Antibody	44.39
56	Antibody	42.10
57	Antibody	41.92

Shapiro–Wilk tests revealed non-normal distributions for the PreAbs.Antibody ($W = 0.8158$, $p < 0.001$) and Antibody groups ($W = 0.8845$, $p = 0.015$), while the No.Antibody group showed a normal distribution ($W = 0.8557$, $p = 0.051$). Due to the presence of non-normal data, non-parametric analysis was employed for all pairwise comparisons.

The mean Ct values were No.Antibody: 40.7 ± 2.3, PreAbs.Antibody: 35.6 ± 8.1, and Antibody: 35.6 ± 8.5. Pairwise comparisons using Mann–Whitney U tests revealed no significant differences between any groups: PreAbs.Antibody vs. No.Antibody ($W = 109$, $p = 0.430$), Antibody vs. No.Antibody ($W = 92$, $p = 0.281$), and PreAbs.Antibody vs. Antibody ($W = 259.5$, $p = 0.930$).

These findings indicate that while both antibody treatments showed numerically lower Ct values compared to the no-antibody control, the differences were not statistically significant, suggesting comparable performance between pre-absorbed and non-treated antisera under these experimental conditions.

3.2.2. Experiment 2b: Comparison of Reverse Transcriptases

To assess the performance of the laboratory-produced Mashup RTase relative to commercial SuperScript II (SSII), cycle threshold (Ct) values were compared between the two groups using standard samples. A total of 28 samples were analyzed, including 24 standard samples and four negative controls; the negative controls were excluded from the statistical analysis comparing reverse transcriptase performance (Figure 3, Table 3).

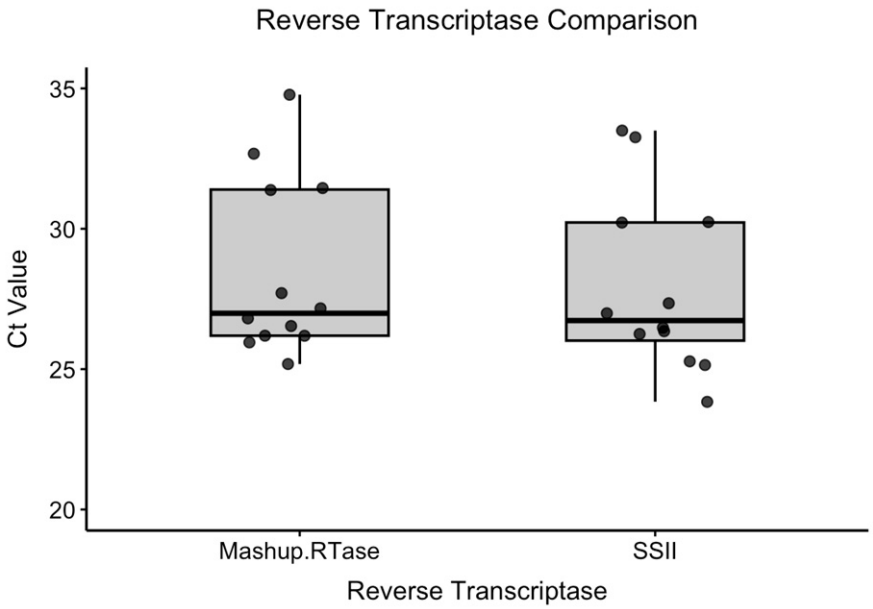


Figure 3. Comparison of reverse transcriptases for immunocapture RT-qPCR detection of DWV-A. Cycle threshold (Ct) values comparing laboratory-produced Mashup RTase and commercial SuperScript II (SSII) using standard samples. Box plots show median (horizontal line), interquartile range (box), and individual data points overlaid. Shapiro–Wilk tests revealed non-normal distribution for Mashup RTase ($p = 0.028$), necessitating non-parametric analysis. Mann–Whitney U tests showed no significant difference between reverse transcriptases (W = 80, $p = 0.665$), $n = 12$ per group.

Table 3. Comparison of reverse transcriptase performance in RT-qPCR detection of DWV-A. Cycle threshold (Ct) values comparing laboratory-produced Mashup RTase and commercial SuperScript II reverse transcriptases.

Sample	Transcriptase	Ct Value
1	Mashup.RTase	25.95
2	Mashup.RTase	25.18
3	SSII	26.35
4	SSII	23.84
5	Mashup.RTase	26.19
6	Mashup.RTase	27.70
7	SSII	26.99
8	SSII	27.34
9	Mashup.RTase	31.45
10	Mashup.RTase	34.78
11	SSII	33.50
12	SSII	33.26

Table 3. *Cont.*

Sample	Transcriptase	Ct Value
13	Mashup.RTase	49.04
14	Mashup.RTase	47.35
15	Mashup.RTase	26.19
16	Mashup.RTase	26.53
17	SSII	25.14
18	SSII	25.28
19	Mashup.RTase	26.81
20	Mashup.RTase	27.17
21	SSII	26.26
22	SSII	26.47
23	Mashup.RTase	32.68
24	Mashup.RTase	31.38
25	SSII	30.24
26	SSII	30.22
27	Mashup.RTase	43.90
28	SSII	45.78

Shapiro–Wilk tests revealed a non-normal distribution for Mashup RTase (W = 0.8407, $p = 0.028$), while SSII showed a normal distribution (W = 0.8874, $p = 0.109$). Due to the presence of non-normal data, non-parametric analysis was employed.

The mean Ct values were Mashup RTase: 28.5 ± 3.2 and SSII: 27.9 ± 3.2. Mann–Whitney U tests revealed no significant difference between RT types (W = 80, $p = 0.665$). These findings support the use of Mashup RTase as a cost-effective, laboratory-produced enzyme for large-scale DWV surveillance programs, with performance comparable to commercial SuperScript II.

3.3. Experiment 3: Method Validation

3.3.1. 3a: Sensitivity Comparison

We performed a direct comparison of the IC-RT-PCR and TRIzol® methods using identical bee samples ($n = 20$) (Figure 4, Table 4).

Shapiro–Wilk tests revealed non-normal distributions for both the TRIzol® (W = 0.6693, $p < 0.001$) and Immunocapture methods (W = 0.7333, $p < 0.001$), necessitating non-parametric analysis. Spearman correlation analysis revealed a strong positive correlation (rho = 0.821, $R^2 = 0.675$, $p < 0.001$). Linear regression analysis confirmed an excellent agreement between methods ($R^2 = 0.958$, $p < 0.001$).

Paired comparison using Wilcoxon signed-rank tests revealed a significant difference between methods (V = 3, $p < 0.001$), with TRIzol® yielding consistently lower Ct values (mean difference = −5.99 ± 3.71). The overall means were TRIzol® 20.9 ± 9.2 and IC-RT-PCR 26.9 ± 5.8. Despite this systematic difference, the strong correlation indicates excellent proportional agreement between methods across the full range of viral loads tested (Ct values 15–35).

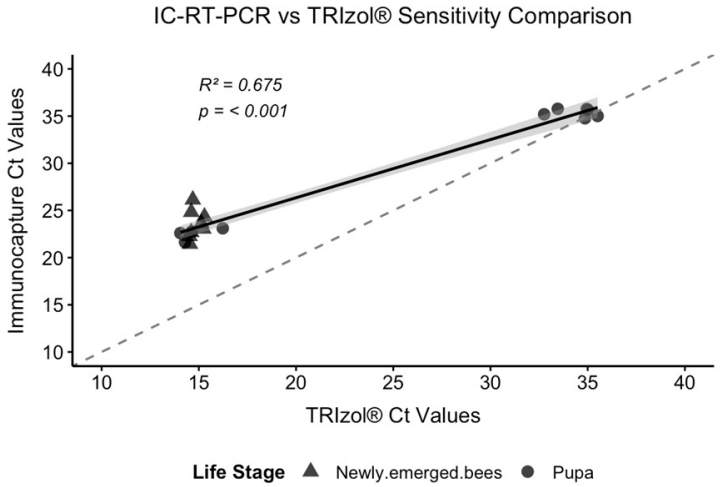


Figure 4. Sensitivity comparison between IC-RT-PCR and TRIzol® methods. Correlation plot showing cycle threshold (Ct) values from paired samples analyzed by both TRIzol® RNA extraction (*x*-axis) and immunocapture RT-qPCR (*y*-axis). Different symbols represent life stages: circles (Pupa, $n = 10$) and triangles (Newly emerged bees, $n = 10$). The solid black line shows linear regression fit with 95% confidence interval (gray shading). The dashed gray line represents perfect 1:1 agreement (y = x). Spearman correlation analysis revealed strong positive correlation (rho = 0.821, $R^2 = 0.675$, $p < 0.001$). Linear regression showed excellent agreement ($R^2 = 0.958$, $p < 0.001$) despite TRIzol® yielding systematically lower Ct values. $n = 20$ paired samples.

Table 4. Method comparison across bee life stages for detection of DWV-A. Ct values for pupae and newly emerged bees using TRIzol® versus immunocapture extraction.

Sample	Life Stage	TRIzol® Ct	Immunocapture Ct
1	Pupa	16.23	23.11
2	Pupa	14.29	21.63
3	Pupa	14.05	22.60
4	Pupa	14.63	22.76
5	Pupa	32.76	35.19
6	Pupa	33.46	35.77
7	Pupa	34.95	35.75
8	Pupa	35.51	35.01
9	Pupa	35.01	35.67
10	Pupa	34.86	34.77
11	Newly.emerged.bees	15.13	23.64
12	Newly.emerged.bees	14.61	22.69
13	Newly.emerged.bees	14.69	26.14
14	Newly.emerged.bees	15.29	24.34
15	Newly.emerged.bees	14.61	24.83
16	Newly.emerged.bees	14.52	22.27
17	Newly.emerged.bees	14.54	21.45
18	Newly.emerged.bees	15.23	23.06
19	Newly.emerged bees	14.16	23.24
20	Newly.emerged bees	20.04	24.44

3.3.2. 3b: Life Stage Comparison

We evaluated the method performance across two honey bee life stages using paired samples: pupae (n = 10) and newly emerged bees (n = 10) analyzed with both the TRIzol® and IC-RT-PCR methods (Figure 5, Table 4).

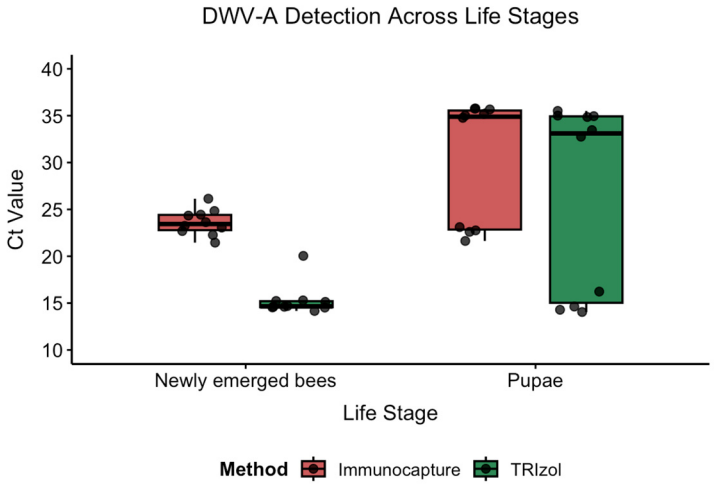


Figure 5. Life stage comparison of DWV-A detection methods. Cycle threshold (Ct) values comparing pupae and newly emerged honey bees using both TRIzol® (green) and immunocapture RT-qPCR (red) methods. Box plots show median, quartiles, and individual data points for each life stage × method combination. Both methods detected the same biological pattern, with newly emerged bees showing numerically lower Ct values (higher viral loads) than pupae, though the differences were not statistically significant due to high variability within groups. TRIzol® consistently yielded lower Ct values than IC-RT-PCR, with the difference being more pronounced in newly emerged bees (8.3 Ct) than pupae (3.7 Ct). n = 10 per life stage, 20 total paired samples.

Statistical Analysis: Shapiro–Wilk tests revealed non-normal distributions for three of four groups (Newly.emerged.bees-TRIzol: W = 0.561, $p < 0.001$; Pupa-Immunocapture: W = 0.702, $p < 0.001$; Pupa-TRIzol: W = 0.714, $p = 0.001$), with only Newly.emerged.bees-Immunocapture showing a normal distribution (W = 0.988, $p = 0.994$), necessitating non-parametric analysis.

Results: Both methods detected numerical differences in viral loads between life stages, with newly emerged bees showing lower Ct values (higher viral loads) than pupae. For TRIzol®, the mean difference was 11.3 Ct units (pupae: 26.6 ± 10.2 vs. newly emerged: 15.3 ± 1.7), while IC-RT-PCR showed a 6.6 Ct unit difference (pupae: 30.2 ± 6.7 vs. newly emerged: 23.6 ± 1.4). However, Mann–Whitney U tests revealed that these life stage differences were not statistically significant for either method (TRIzol®: W = 75, $p = 0.064$; IC-RT-PCR: W = 70, $p = 0.143$).

Method Comparison Within Life Stages: Method comparisons within each life stage showed no significant difference in pupae (W = 30.5, $p = 0.151$), but a highly significant difference in newly emerged bees (W = 0, $p < 0.001$), with TRIzol® yielding consistently lower Ct values (8.3 Ct difference) for this life stage.

These findings indicate that while both methods detected the same biological pattern (higher viral loads in newly emerged bees), the high variability within groups, particularly in pupae, limited the statistical significance, despite substantial numerical differences.

3.4. Experiment 4: Virus Delivery Assessment

To compare the sensitivity of TRIzol®-based RNA extraction and immunocapture RT-qPCR in detecting viral genome equivalents across different infection routes and doses, we

analyzed Ct values obtained from newly emerged bees exposed to either oral or injection-based infections (Figure 6, Table 5).

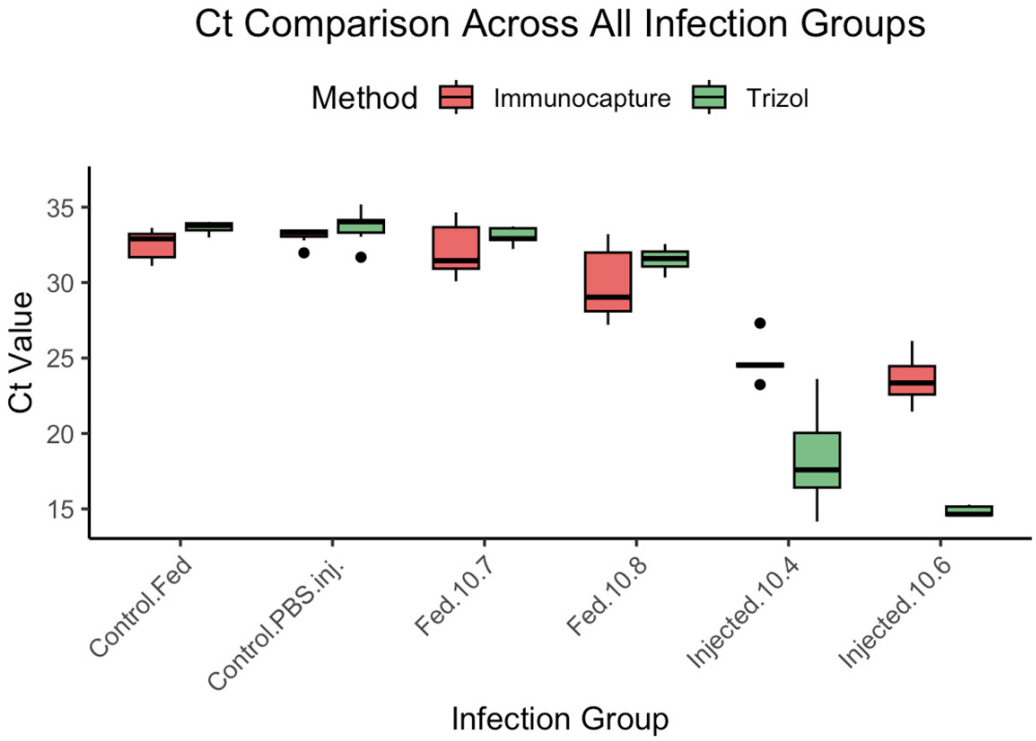


Figure 6. Virus delivery assessment comparing TRIzol® and immunocapture RT-qPCR across infection routes and doses. Cycle threshold (Ct) values for different treatment groups: Controls (Control.Fed, Control.PBS.inj.), oral infections (Fed.10.7, Fed.10.8 representing 10^7 and 10^8 genome equivalents), and injection infections (Injected.10.4, Injected.10.6 representing 10^4 and 10^6 genome equivalents). Box plots show median, quartiles, and outliers for TRIzol® (green) and Immunocapture (red) methods. TRIzol® demonstrated markedly superior sensitivity for injection-based infections, particularly at lower doses, while both methods showed comparable performance for oral infections at higher doses.

Statistical Analysis: Shapiro–Wilk tests revealed non-normal distributions for two treatment groups (Control.PBS.inj.-Immunocapture: W = 0.737, p = 0.009; Injected.10.6-TRIzol®: W = 0.802, p = 0.030), while the other groups showed normal distributions, necessitating non-parametric analysis for affected comparisons.

Results by Infection Route:

Oral Infections (Fed groups):

- At 10^7 genome equivalents (Fed.10.7): TRIzol® 33.1 ± 0.6 vs. IC-RT-PCR 32.2 ± 1.9 (no significant difference expected based on overlapping ranges)
- At 10^8 genome equivalents (Fed.10.8): TRIzol® 31.5 ± 0.8 vs. IC-RT-PCR 30.0 ± 2.5 (IC-RT-PCR showing slightly lower Ct values)

Injection Infections (Injected groups):

- At 10^4 genome equivalents (Injected.10.4): TRIzol® 18.4 ± 3.6 vs. IC-RT-PCR 24.8 ± 1.5 (substantial difference, TRIzol® more sensitive)
- At 10^6 genome equivalents (Injected.10.6): TRIzol® 14.8 ± 0.3 vs. IC-RT-PCR 23.6 ± 1.5 (pronounced difference, TRIzol® markedly more sensitive)

Controls:

- Control.Fed: TRIzol® 33.6 ± 0.4 vs. IC-RT-PCR 32.5 ± 1.0
- Control.PBS.inj.: TRIzol® 33.7 ± 1.1 vs. IC-RT-PCR 33.1 ± 0.6

Table 5. Effect of virus delivery route on detection method performance. Ct values for oral versus injection infections using TRIzol® and immunocapture extraction.

Sample	Treatment	TRIzol® Ct	Immunocapture Ct
1	Control.Fed	33.40	31.22
2	Control.Fed	33.53	32.90
3	Control.Fed	32.99	33.33
4	Control.Fed	33.95	32.14
5	Control.Fed	33.79	31.10
6	Control.Fed	33.90	33.63
7	Control.Fed	34.00	33.12
8	Control.PBS.inj.	34.15	31.97
9	Control.PBS.inj.	34.14	33.31
10	Control.PBS.inj.	35.18	32.79
11	Control.PBS.inj.	33.03	33.30
12	Control.PBS.inj.	34.03	33.47
13	Control.PBS.inj.	33.59	33.41
14	Control.PBS.inj.	31.68	33.48
15	Fed.10.7	32.22	33.67
16	Fed.10.7	33.60	34.65
17	Fed.10.7	32.91	30.08
18	Fed.10.7	32.83	31.45
19	Fed.10.7	33.72	30.92
20	Fed.10.8	31.59	30.95
21	Fed.10.8	32.55	28.43
22	Fed.10.8	30.97	33.21
23	Fed.10.8	32.21	33.03
24	Fed.10.8	31.90	29.03
25	Fed.10.8	30.33	27.20
26	Fed.10.8	31.16	27.77
27	Injected.10.4	14.16	23.24
28	Injected.10.4	20.04	24.44
29	Injected.10.4	16.42	24.62
30	Injected.10.4	17.59	27.31
31	Injected.10.4	23.62	24.54
32	Injected.10.6	15.13	23.64
33	Injected.10.6	14.61	22.69
34	Injected.10.6	14.69	26.14
35	Injected.10.6	15.29	24.34
36	Injected.10.6	14.61	24.83
37	Injected.10.6	14.52	22.27
38	Injected.10.6	14.54	21.45
39	Injected.10.6	15.23	23.06

4. Discussion

The development of cost-effective and scalable tools for DWV detection is essential for both research and field-level surveillance. Our findings demonstrate that immunocapture RT-qPCR (IC-RT-PCR) offers a practical alternative to conventional RNA extraction methods for specific applications, though with important limitations that must be considered for appropriate implementation.

4.1. Antibody Performance and Protocol Simplification

Contrary to initial expectations, pre-absorption of antisera did not significantly improve detection performance compared to non-treated antibodies. While this finding initially appeared to contradict the theoretical benefits of reducing background binding, it actually provides a practical advantage by eliminating an unnecessary preparation step. The lack of significant differences between antibody treatments suggests that the immunocapture process is sufficiently robust to function effectively without extensive antibody optimization, simplifying implementation for routine use.

The 1:1000 antisera dilution emerged as the optimal choice, not due to statistical superiority, but rather because of its practical advantages, including reduced antibody consumption and lower variability. This finding supports the scalability of the method for large surveillance programs where antibody costs could become prohibitive.

4.2. Reverse Transcriptase Equivalency and Cost Implications

The validation of laboratory-produced Mashup RTase as equivalent to commercial SuperScript II addresses a critical cost barrier for large-scale implementation. With potential cost savings of 75–85% in RT expenses, this finding significantly enhances the economic feasibility of the IC-RT-PCR approach for surveillance programs.

Cost Analysis Example: For a surveillance program processing 1000 samples annually, commercial SuperScript II costs approximately USD 2000–2500 per year for RT alone. Laboratory-produced Mashup RTase reduces this to USD 300–500 annually, yielding savings of USD 1500–2200 per year. Combined with elimination of hazardous waste disposal costs (USD 500–1000 annually) and reduced safety infrastructure requirements, the total cost savings could exceed USD 2000–3000 per year for medium-scale operations.

The comparable performance between enzymes ($p = 0.665$) validated the use of in-house produced RT, while providing greater supply chain control and customization opportunities. For laboratories processing > 500 samples annually, the initial investment in RT production capabilities would typically achieve cost recovery within 6–12 months.

4.3. Sensitivity Analysis and Method Limitations

While IC-RT-PCR demonstrated strong correlation with TRIzol® extraction (rho = 0.821), the method yielded consistently higher Ct values (mean difference = 5.99 ± 3.71), indicating reduced sensitivity compared to the gold standard. This difference likely reflects inherent losses during the immunocapture washing steps and suggests that IC-RT-PCR is most suitable for applications where moderate to high viral loads are expected, such as surveillance of symptomatic colonies or monitoring treatment efficacy.

The excellent linear relationship ($R^2 = 0.958$) validates IC-RT-PCR as a reliable method for comparative viral load assessment, even though the absolute sensitivity differed from TRIzol®. The preserved proportionality across viral loads and life stages confirms that biological differences are accurately detected by both methods.

Based on these findings, IC-RT-PCR is recommended for large-scale surveillance programs where safety, cost, and throughput are prioritized over maximal sensitivity.

For detection of low-level infections or research requiring precise quantification, TRIzol® extraction remains the preferred method.

4.4. Life Stage Comparison

Biological Relevance: Despite the lack of statistical significance, both methods consistently detected higher viral loads in newly emerged bees compared to pupae, with effect sizes (6–11 Ct differences) that were biologically meaningful. The high variability within pupal samples likely reflects natural heterogeneity in infection timing and viral replication during development.

Method Selection Guidance: The significant difference in methods in newly emerged bees ($p < 0.001$) but not in pupae ($p = 0.151$) suggests that TRIzol® provides greater sensitivity advantages when viral loads are higher and more consistent. For surveillance of mixed-age populations, IC-RT-PCR may provide adequate information for detecting general infection patterns.

Study Design Implications: The high variability in pupal samples suggests that larger sample sizes or more precise developmental staging may be needed to achieve statistical significance in life stage comparisons. Alternatively, focusing on newly emerged bees may provide more consistent and statistically powerful results.

4.5. Route-Specific Performance

The dramatic difference in method performance between oral and injection routes suggests that the immunocapture method may be less effective at detecting systemically distributed virus compared to locally concentrated infections. This finding has important implications for surveillance program design, where the expected infection route may influence method selection.

Sensitivity Thresholds: TRIzol® extraction demonstrated superior sensitivity for detecting low-level systemic infections introduced by injection, with Ct values 6–9 cycles lower than IC-RT-PCR. This difference likely reflects the immunocapture method's inherent losses during washing steps, which become more critical when initial viral loads are low.

Practical Applications: For field surveillance where natural oral infections predominate and viral loads are typically moderate to high, IC-RT-PCR provides adequate sensitivity, with significant cost and safety advantages. However, for research applications requiring detection of experimentally induced low-level infections or for diagnostic confirmation of suspected cases, TRIzol® extraction remains the preferred method.

4.6. Practical Applications and Method Selection Guidelines

Based on our comprehensive analysis, clear guidelines emerge for appropriate IC-RT-PCR application:

Recommended for

- Large-scale surveillance programs prioritizing safety, cost, and throughput
- Monitoring moderate to high viral loads in naturally infected colonies
- Screening programs where relative viral load assessment is sufficient
- Field applications where hazardous chemical use is prohibited
- High-throughput scenarios requiring automation compatibility

Not recommended for

- Detection of low-level experimental infections
- Research requiring maximal analytical sensitivity
- Diagnostic confirmation of suspected cases with low viral loads
- Studies requiring precise absolute quantification

4.7. Methodological Considerations and Future Directions

Several methodological improvements could enhance IC-RT-PCR performance. The current 18 h immunocapture incubation, while optimized for sensitivity, limits rapid diagnostic applications. Future work should investigate shorter incubation times and their impact on detection limits. Additionally, the method's current limitation to DWV-A detection represents a significant constraint given the epidemiological importance of other DWV variants, particularly DWV-B.

Integration with portable detection platforms represents a promising development path. The simplified workflow and reduced hazardous chemical requirements make IC-RT-PCR particularly suitable for field-deployable diagnostic systems. However, such applications would need to carefully consider the sensitivity limitations identified in this study.

4.8. Economic and Safety Benefits

The elimination of phenol-chloroform extraction provides substantial safety benefits, particularly for large-scale screening programs. Cost analysis suggests significant savings through reduced chemical purchases, waste disposal costs, and safety infrastructure requirements. For surveillance programs processing hundreds or thousands of samples, these savings could be substantial, while providing adequate analytical performance for program objectives.

4.9. Study Limitations

Several limitations merit acknowledgment:

1. Single virus focus: Validation was limited to DWV-A, restricting applicability to comprehensive viral screening
2. Laboratory conditions: All validations were performed under controlled laboratory conditions; requirement for field validation remains
3. Sample matrix: Testing was limited to honey bee homogenates; performance with other sample types (bee bread, honey, etc.) requires separate validation
4. Storage stability: Long-term stability of immunocaptured samples was not evaluated
5. Cross-reactivity: Comprehensive testing against related viruses was not performed

5. Conclusions

The IC-RT-PCR method represents a significant advance in DWV detection methodology when applied appropriately to its intended use cases. Our comprehensive validation demonstrates that while the method does not achieve the absolute sensitivity of TRIzol® extraction, it provides reliable, proportional viral load assessment, with substantial practical advantages.

Key findings:

1. Method validation: IC-RT-PCR shows strong correlation (rho = 0.821) with TRIzol® extraction but with reduced absolute sensitivity (~6 Ct difference)
2. Cost-effectiveness: Combination with laboratory-produced RT and simplified antibody protocols provides substantial cost savings for large-scale applications
3. Route-dependent performance: Method performs adequately for oral infections at moderate to high doses but shows limitations for low-level systemic infections
4. Safety advantages: Elimination of hazardous chemical extraction provides significant safety benefits for high-throughput applications

Practical impact: This method fills an important gap for surveillance applications where safety, cost, and throughput are prioritized over maximal sensitivity. For research

applications requiring detection of low-level infections or precise quantification, TRIzol® extraction remains the preferred approach.

Future directions: Continued development should focus on expanding virus specificity to include other DWV variants, optimizing incubation conditions for reduced processing time, and validation under field conditions. Integration with portable diagnostic platforms represents a particularly promising application given the method's simplified workflow and reduced infrastructure requirements.

The honest assessment of method capabilities and limitations provided in this study should guide appropriate implementation and prevent misapplication in contexts requiring maximal analytical sensitivity. When applied within its validated performance envelope, IC-RT-PCR offers a valuable tool for advancing DWV surveillance capabilities, while significantly reducing associated costs and safety risks.

Author Contributions: Conceptualization, K.C. and E.V.R.; methodology, K.C., E.V.R. and J.T.; validation, K.C. and J.T.; formal analysis, K.C. and J.T.; investigation, K.C.; resources, J.D.E. and E.V.R.; data curation, K.C.; writing—original draft preparation, K.C.; writing—review and editing, K.C., J.T., E.V.R. and J.D.E.; visualization, K.C. and J.T.; supervision, J.D.E.; project administration, J.D.E.; funding acquisition, J.D.E. and E.V.R. All authors have read and agreed to the published version of the manuscript.

Funding: This research was funded by USDA-NIFA, grant number 2021-67013-33560 for E.V.R.

Institutional Review Board Statement: Not applicable.

Informed Consent Statement: Not applicable.

Data Availability Statement: Data are contained within the article. The original contributions presented in this study are included in the article. Further inquiries can be directed to the corresponding author.

Acknowledgments: During the preparation of this manuscript, the author K.C. used ChatGPT (GPT-4-turbo, OpenAI, accessed April 2025) for grammar, editing, and visualization assistance. Statistical analysis revisions were conducted with assistance from Claude AI (Sonnet 4, Anthropic, accessed June 2025) to ensure proper normality testing and appropriate statistical test selection. The authors have reviewed and edited all AI-assisted content and take full responsibility for the scientific accuracy and integrity of this publication. We thank the reviewers for their constructive feedback that led to significant improvements in statistical rigor and methodological presentation.

Conflicts of Interest: The authors declare no conflicts of interest. The funders had no role in the design of the study; in the collection, analyses, or interpretation of data; in the writing of the manuscript; or in the decision to publish the results.

References

1. Lanzi, G.; De Miranda, J.R.; Boniotti, M.B.; Cameron, C.E.; Lavazza, A.; Capucci, L.; Camazine, S.M.; Rossi, C. Molecular and biological characterization of deformed wing virus of honeybees (*Apis mellifera* L.). *J. Virol.* **2006**, *80*, 4998–5009. [CrossRef] [PubMed]
2. Francis, R.M.; Nielsen, S.L.; Kryger, P. Varroa-virus interaction in collapsing honey bee colonies. *PLoS ONE* **2013**, *8*, e57540. [CrossRef] [PubMed]
3. Dainat, B.; Evans, J.D.; Chen, Y.P.; Gauthier, L.; Neumann, P. Dead or alive: Deformed wing virus and Varroa destructor reduce the life span of winter honeybees. *Appl. Environ. Microbiol.* **2012**, *78*, 981–987. [CrossRef] [PubMed]
4. Martin, S.J.; Highfield, A.C.; Brettell, L.; Villalobos, E.M.; Budge, G.E.; Powell, M.; Nikaido, S.; Schroeder, D.C. Global honey bee viral landscape altered by a parasitic mite. *Science* **2012**, *336*, 1304–1306. [CrossRef] [PubMed]
5. Schroeder, D.C.; Martin, S.J. Deformed wing virus: The main suspect in unexplained honeybee deaths worldwide. *Virulence* **2012**, *3*, 589–591. [CrossRef] [PubMed]
6. Ryabov, E.V.; Wood, G.R.; Fannon, J.M.; Moore, J.D.; Bull, J.C.; Chandler, D.; Mead, A.; Burroughs, N.; Evans, D.J. A virulent strain of deformed wing virus (DWV) of honeybees (*Apis mellifera*) prevails after Varroa destructor-mediated, or in vitro, transmission. *PLoS Pathog.* **2014**, *10*, e1004230. [CrossRef] [PubMed]

7. Evans, J.D.; Banmeke, O.; Palmer-Young, E.C.; Chen, Y.; Ryabov, E.V. Beeporter: Tools for high-throughput analyses of pollinator-virus infections. *Mol. Ecol. Resour.* **2022**, *22*, 978–987. [CrossRef] [PubMed]
8. Clark, M.F.; Adams, A. Characteristics of the microplate method of enzyme-linked immunosorbent assay for the detection of plant viruses. *J. Gen. Virol.* **1977**, *34*, 475–483. [CrossRef] [PubMed]
9. Angira, A.; Baranwal, V.; Ranjan, A.; Choudhary, N. Optimization of DAC-ELISA and IC-RT-PCR using the developed polyclonal antibody and one-step RT-PCR assays for detection of Indian citrus ringspot virus in kinnow orange of Punjab, India. *J. Virol. Methods* **2024**, *329*, 114972. [CrossRef] [PubMed]
10. Chikh-Ali, M.; Daniel, J.; Aslam, H.M.U.; Agindotan, B.; Charkowski, A.O. Development of a Duplex Immunocapture Reverse-Transcription Quantitative Polymerase Chain Reaction for Large-Scale Detection of Potato Mop-Top Virus in Dormant Potato Tubers. *Plant Dis.* **2025**, *109*, 1354–1358. [CrossRef] [PubMed]
11. Mumford, R.; Seal, S. Rapid single-tube immunocapture RT-PCR for the detection of two yam potyviruses. *J. Virol. Methods* **1997**, *69*, 73–79. [CrossRef] [PubMed]
12. Mordecai, G.J.; Wilfert, L.; Martin, S.J.; Jones, I.M.; Schroeder, D.C. Diversity in a honey bee pathogen: First report of a third master variant of the Deformed Wing Virus quasispecies. *ISME J.* **2016**, *10*, 1264–1273. [CrossRef] [PubMed]
13. Wilfert, L.; Long, G.; Leggett, H.; Schmid-Hempel, P.; Butlin, R.; Martin, S.; Boots, M. Deformed wing virus is a recent global epidemic in honeybees driven by Varroa mites. *Science* **2016**, *351*, 594–597. [CrossRef] [PubMed]
14. Nazzi, F.; Le Conte, Y. Ecology of Varroa destructor, the major ectoparasite of the western honey bee, Apis mellifera. *Annu. Rev. Entomol.* **2016**, *61*, 417–432. [CrossRef] [PubMed]
15. de Miranda, J.R.; Genersch, E. Deformed wing virus. *J. Invertebr. Pathol.* **2010**, *103*, S48–S61. [CrossRef] [PubMed]
16. Yue, C.; Genersch, E. RT-PCR analysis of Deformed wing virus in honeybees (*Apis mellifera*) and mites (*Varroa destructor*). *J. Gen. Virol.* **2005**, *86*, 3419–3424. [CrossRef] [PubMed]
17. Fannon, J.M.; Ryabov, E.V. Iflavirus (Deformed wing virus). In *Molecular Detection of Animal Viral Pathogens*; Routledge: England, UK, 2016; pp. 37–46.
18. Ryabov, E.V.; Christmon, K.; Heerman, M.C.; Posada-Florez, F.; Harrison, R.L.; Chen, Y.; Evans, J.D. Development of a honey bee RNA virus vector based on the genome of a deformed wing virus. *Viruses* **2020**, *12*, 374. [CrossRef] [PubMed]
19. Mashup RT Purification Version 1.2. Available online: https://pipettejockey.com/2018/09/06/mashup-rt-purify-your-own-reverse-transcriptase-beta-testing-phase/ (accessed on 3 July 2020).

Disclaimer/Publisher's Note: The statements, opinions and data contained in all publications are solely those of the individual author(s) and contributor(s) and not of MDPI and/or the editor(s). MDPI and/or the editor(s) disclaim responsibility for any injury to people or property resulting from any ideas, methods, instructions or products referred to in the content.